Experimental Evidence of the Molecular and Macroscopic Origins of Circular Dichroism in Chiral Metal-Halide Networks

Alexandre Abhervé

ADVANCED OPTICAL MATERIALS
www.advopticalmat.de

Experimental Evidence of the Molecular and Macroscopic Origins of Circular Dichroism in Chiral Metal-Halide Networks

Alexandre Abhervé

Clockwise or counter-clockwise spin coating? In the current hot research topic of chiral metal-halide semiconductors, several investigations have been undertaken in order to reveal their natural optical activity and have reported dissymmetry factors (g_{abs}) for thin films of many hybrid compounds, usually without considering the macroscopic anisotropies inherent to solid-state samples. Yet, CD in the solid state can be strongly modulated by the co-existence of linear dichroism (LD) and linear birefringence (LB). Theoretical studies recently revealed the importance of such macroscopic interferences in the CD response of solid-state samples, often referred as symmetric (sLDLB) and antisymmetric (aLDLB) effects. Based on the newly synthesized one-dimensional lead-halide networks of formula (*S*/*R*-HP1A)$PbBr_3$ and (*S*/*R*-HP1A)PbI_3, an experimental method to accurately discriminate between CD, sLDLB and aLDLB in chiral metal-halide networks is here presented. The main experimental conditions influencing sLDLB and aLDLB amplitude are also highlighted, such as the concentration of the precursor solution and the spin-coating rotation direction, finally providing a complete experimental guide for the forthcoming chiroptical investigations of such important family of chiral hybrid materials.

1. Introduction

The recent development of chiral metal-halide semiconductors, such as chiral perovskites,[1] allowed the characterization of their chiroptical properties by circular dichroism (CD),[2] circularly polarized luminescence (CPL)[3] and non-linear optics such as CD-dependent single-harmonic generation (SHG-CD).[4] Based on the first results reported in the last six years, some comparative studies tried to evaluate the potential of this class of materials for chiroptical applications.[5] It appeared that one-dimensional (1D) networks presented g_{abs} factors of between 10^{-3} – 10^{-1}, one to two orders of magnitude higher than two-dimensional (2D) compounds ($10^{-4} < g_{abs} < 10^{-3}$). On the other hand, iodide-based compounds presented slightly higher g_{abs} factors than bromide-based counterparts. However, these properties were evaluated either on bulk crystals[6] or on crystalline thin films,[7] most of the time without considering the macroscopic interferences that could modulate the CD response in solid-state samples. For instance, the record g_{abs} factor of 0.04 reported in a 1D lead-iodide compound was actually obtained from a mixed composition of CD-active 1D (*S*/*R*-NEA)PbI_3 and achiral 3D $MAPbI_3$ in the thin films, and neither the crystal structure or the co-assembly of the composite could be described.[8] Furthermore, such samples were prepared starting with saturated precursor solutions which probably place the absorbance of the resulting thin films over the accuracy window of the CD spectroscopy technique. Controlling the purity and appropriateness of CD measurements is of paramount importance especially when dealing with solid-state samples with strong anisotropy. Indeed, it has been recently evidenced for organic molecules that linear dichroism (LD) and linear birefringence (LB) can strongly interact locally inside the thin film, and their contribution along the *xy* plane orthogonal to the light propagation can be detected as circular absorption.[9] Considering LD and LB measured along the *x*-*y* axes, those measured along the bisectors of *x*-*y* axes (LD' and LB'), the rotation angle of the sample around the optical axis (θ), together with some other constants associated to the detection system (residue birefringence α, azimuth angle a, P^2_x and P^2_y related to the transmittance of the detector), the experimentally measured CD signal can be expressed as

$$CD_{total} = CD_{iso} + \frac{1}{2}\left(LD' \cdot LB - LB' \cdot LD\right) + \left(-LD\cos 2\theta + LD'\sin 2\theta\right)\sin\alpha + \left(P^2_x - P^2_y\right)\sin 2a\left(-LB\cos 2\theta + LB'\sin 2\theta\right) \quad (1)$$

A. Abhervé
Laboratoire
MOLTECH-Anjou
UMR 6200
CNRS
UNIV
Angers
2 Boulevard Lavoisier, ANGERS, Cedex 49045, France
E-mail: alexandre.abherve@univ-angers.fr

The ORCID identification number(s) for the author(s) of this article can be found under https://doi.org/10.1002/adom.202400381

DOI: 10.1002/adom.202400381

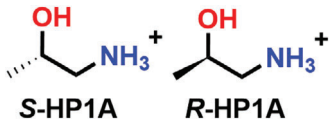

Scheme 1. Structures of the chiral cations.

While the third and fourth terms in equation (1) result in small and easily identified artefacts, the second term in turn can be non-negligible or even predominant over genuine CD_{iso}. This so-called LDLB effect involves pairs of non-parallel transition dipoles when projected in the plane orthogonal to the light propagation. Some experimental studies have demonstrated the macroscopic origins of LDLB[10] and the possibility to isolate this effect from CD_{iso},[11] by measuring the chiroptical response of the thin film in two different configurations, i.e., with the film pointing towards the light source (hereafter called "front position") or toward the detector ("back position"). It was therefore described as antisymmetric with respect to the direction of light propagation. In parallel, the existence of another LDLB contribution was recently demonstrated when considering the helical stacking of the molecules along the light propagation direction.[12] In this theoretical model by Tempelaar et al. (supported by experimental measurements on oligothiophene films), the total LDLB for two nondegenerate transition dipoles n and m could be expressed as

$$LDLB = \xi^2 \omega^2 \sum_{n,m} S_n S_m V_n W_m \left[\frac{1}{2}\sin\left(2\beta_{nm}\right) - \frac{1}{3}\cos\left(2\beta_{nm}\right)\phi\right] \quad (2)$$

where ξ is a constant, ω, V_n and W_m are related to the energy of the transitions, S_n and S_m are the oscillator strengths, β_{nm} the angle between the transition dipoles, and Φ the twist angle between the first and last molecules in the stack (assuming that this angle has a value $\ll 1$). The first term in equation (2) corresponds to the antisymmetric LDLB (hereafter denoted as aLDLB) and changes sign when flipping the sample as a result of the sine function. On the other hand, the second term mainly derives from the helical stacking Φ of a single transition dipole along the light propagation direction, with a cosine function resulting in that case in the conservation of the sign upon sample flipping. Therefore, this term was referred as symmetric LDLB term and is hereafter denoted as sLDLB. All these macroscopic effects are expected to appear in highly crystalline films such as in the case of metal-halide semiconductors. However, the study of macroscopic interferences has been so far largely ignored in this family of materials. Very recently, H. Lu et al. faced this issue and have shown that aLDLB effects tend to increase when decreasing the dimensionality of the network.[13] For instance, the apparent strong g_{abs} factor of 0.1 measured in the first place in the zero-dimensional hybrid compound of formula $(R\text{-MBA})_2CuCl_4$[14] was finally corrected and estimated at 2.5×10^{-3} since the original signal was strongly dominated by the aLDLB term. On the other hand, 1D networks were described to present similar contributions for both CD_{iso} and aLDLB, while in 2D networks the measured signal is dominated by the CD_{iso} term and no macroscopic interference could affect the values of the calculated g_{abs} factors.[15] For example, we very recently reported 2D lead-bromide networks based on the chiral *S*/*R*-2-hydroxy-propyl-1-ammonium (*S*/*R*-HP1A) cations (**Scheme 1**), which presented a pure molecular CD with g_{abs} of about $\pm 10^{-4}$ and high spin polarization in the electron transport.[16] In the present work, the CD characterization of new 1D lead-halide compounds of formula (*S*/*R*-HP1A)$PbBr_3$ and (*S*/*R*-HP1A)PbI_3 is presented. Both compounds have similar crystal structures and only differ from the halide composition. Modulation of the thin film preparation conditions allows to evidence for the first time the presence of both CD, aLDLB and sLDLB in the family of hybrid metal-halide semiconductors. Based on these observations, it is possible to re-investigate the nature of the CD responses in previously reported compounds and to confirm the crucial role of hydrogen-bonding interactions in these organic-inorganic hybrid networks. Finally, a guide for accurately measuring the CD signature in these materials is provided, emphasizing the impact of halide composition, precursor concentration, thin film orientation during CD measurements and, unexpectedly, the direction of the rotation during the spin-coating process.

2. Results and Discussion

2.1. Structures of (*S*/*R*-HP1A)$PbBr_3$ and (*S*/*R*-HP1A)PbI_3

Both bromide and iodide-based compounds crystallize in the non-centrosymmetric polar space group $P2_1$ and are isostructural (Table S1, Supporting Information). Asymmetric units contain two cations and two PbX_3 units (Figure S1, Supporting Information). The 1D network is based on double-chains of edge-sharing PbX_6 octahedra running along the crystallographic [100] direction. The polar axis is thus perpendicular to the propagation of the chains. Both independent octahedra are strongly distorted due to two different Pb–X bond distances (Table S2, Supporting Information). The shortest distance can be found between the metal center and the only terminal halide ion, while the longest distance point towards the center of the double-chain. Numerous N-H···X intermolecular interactions can be observed between cations and the terminal halides (Figure S2, Supporting Information). On the other hand, the equatorial Pb–X bond distances have similar values (from 2.965(8) to 3.109(7) Å in (*S*/*R*-HP1A)$PbBr_3$ and from 3.142(3) to 3.294(2) Å in (*S*/*R*-HP1A)PbI_3). At first, the two pairs of edge-sharing octahedra from both enantiomeric compounds appear to share the same distortions and thus to be superimposable. However, by carefully looking in the equatorial plane, one can observe that the distribution of the bond distances values is clearly inverted between both enantiomeric compounds (**Figure 1**). These mirror-image octahedra clearly highlight the chiral nature of the inorganic network.

These compounds share many similarities such as the crystal structure, symmetry, nature of the metal and of the cation, distortion within the inorganic network, and only differ from each other by the nature of the halide. Therefore, they represent interesting materials to disclose the role of halide composition in the chiroptical properties. Thin films of (*S*/*R*-HP1A)$PbBr_3$ and (*S*/*R*-HP1A)PbI_3 were prepared using the spin-coating method starting from DMF solution of pure crystalline samples, using the typical procedure previously reported (see Supporting Information for experimental procedure). X-ray powder diffraction (XRPD) confirmed the phase and purity for both of the

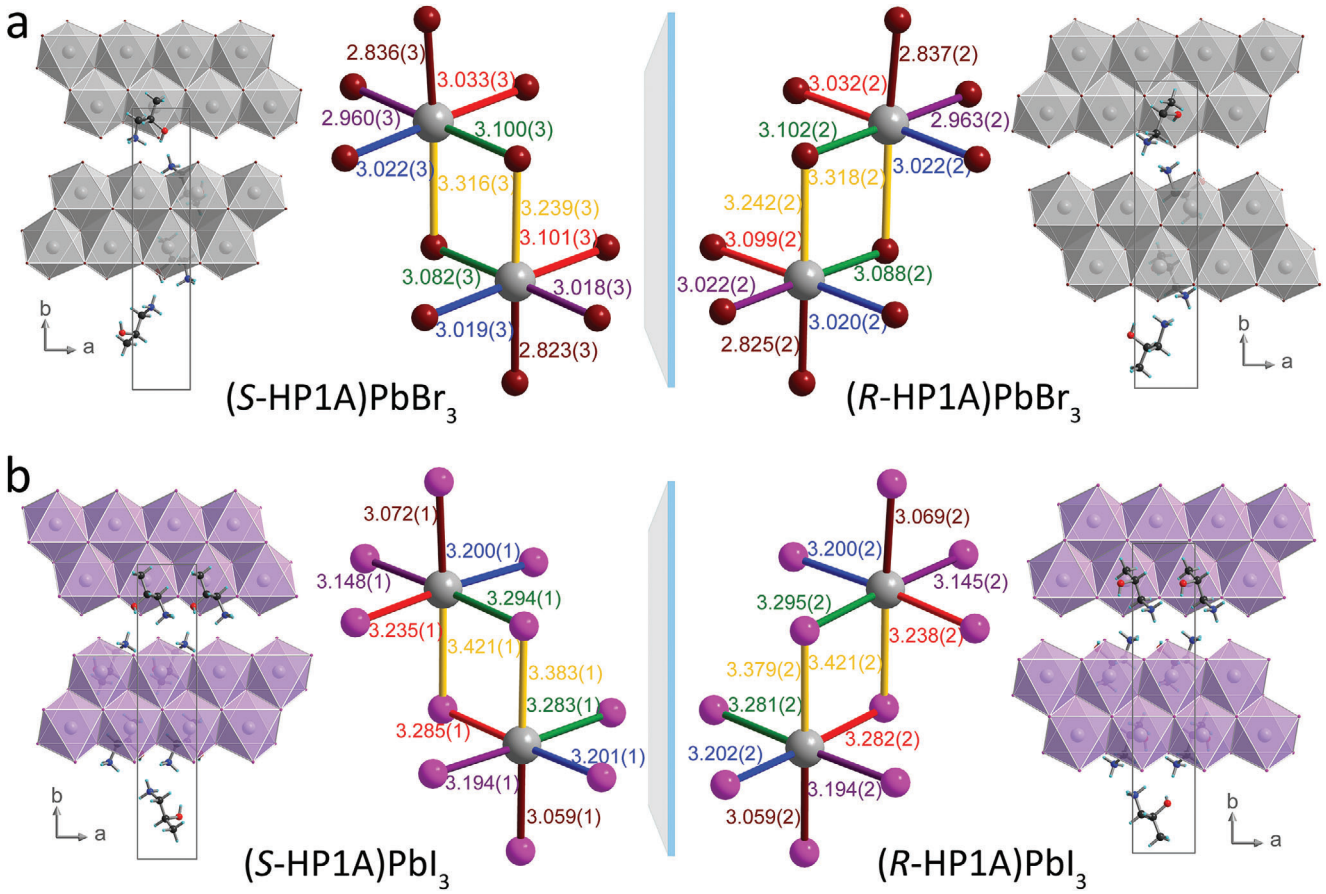

Figure 1. Crystal structures of (*S*/*R*-HP1A)$PbBr_3$ and (*S*/*R*-HP1A)PbI_3. a) View of the unit cell and the two independent edge-sharing octahedra of (*S*-HP1A)$PbBr_3$ (left) and (*R*-HP1A)$PbBr_3$ (right). b) Same for (*S*-HP1A)PbI_3 and (*R*-HP1A)PbI_3. Color code: C (black), H (cyan), N (blue), O (red), Br (brown), I (pink), Pb (grey), $PbBr_6$ unit (grey octahedra), PbI_6 unit (violet octahedra). The longest and shortest apical Pb–X distances are represented in gold and brown, respectively. All equatorial Pb–X bonds are represented in different colors to highlight the chiral nature of the inorganic network.

crystalline powders and in the thin films (Figures S3, S4 and S5, Supporting Information).

2.2. Chiroptical activity in (*S*/*R*-HP1A)$PbBr_3$

CD measurements in transmission mode were first performed by orienting the deposited film towards the light source (i.e., "front" position). The film was rotating along the optical axis and the CD response was measured for eight different azimuth angles θ, with a step of 45° between each measurement (Figure S6, Supporting Information). Indeed, as previously described for organic molecules and coordination complexes, the small artefacts resulting from the third and fourth terms in equation (1) could be corrected by averaging the experimental values obtained at different θ angles. The same procedure was applied for the two enantiomeric compounds, and the averaged spectra are presented in Figure 2a. However, this first series of measurements gave no mirror-image spectra between (*S*-HP1A)$PbBr_3$ and (*R*-HP1A)$PbBr_3$. Although the signals appear at similar wavelengths associated to the excitonic peak of the inorganic 1D network, with a sign inversion between the two enantiomeric compounds, the relative peak intensities were very different from each other. Since they were prepared starting from the same concentration of the precursor solution, thicknesses are expected to be very similar between both films. This is further confirmed by the relative absorbance, the same for both compounds (around 1.1). Using the formula g_{abs} = CD / 32 980 x Abs, it resulted in apparent dissymmetry factors of $+5.10^{-3}$ and -1.10^{-2} for (*S*-HP1A)$PbBr_3$ and (*R*-HP1A)$PbBr_3$, respectively. Very different results were obtained by flipping the sample and measuring the CD spectra in the "back" position (thin film oriented towards the detector), particularly in the case of (*R*-HP1A)$PbBr_3$ for which the spectrum was almost inverted. These results confirm an important contribution of aLDLB effects in these crystalline films. Using the equations

$$CD_{iso} + sLDLB = \frac{1}{2}\left(CD_{front} + CD_{back}\right) \quad (3)$$

$$aLDLB = \frac{1}{2}\left(CD_{front} - CD_{back}\right) \quad (4)$$

it was possible to isolate the contribution of both thickness-independent (CD_{iso} + sLDLB) and thickness-dependent (aLDLB) terms (Figure 2b). As expected, the CD_{iso} + sLDLB display mirror-image spectra between the two enantiomers. This finally

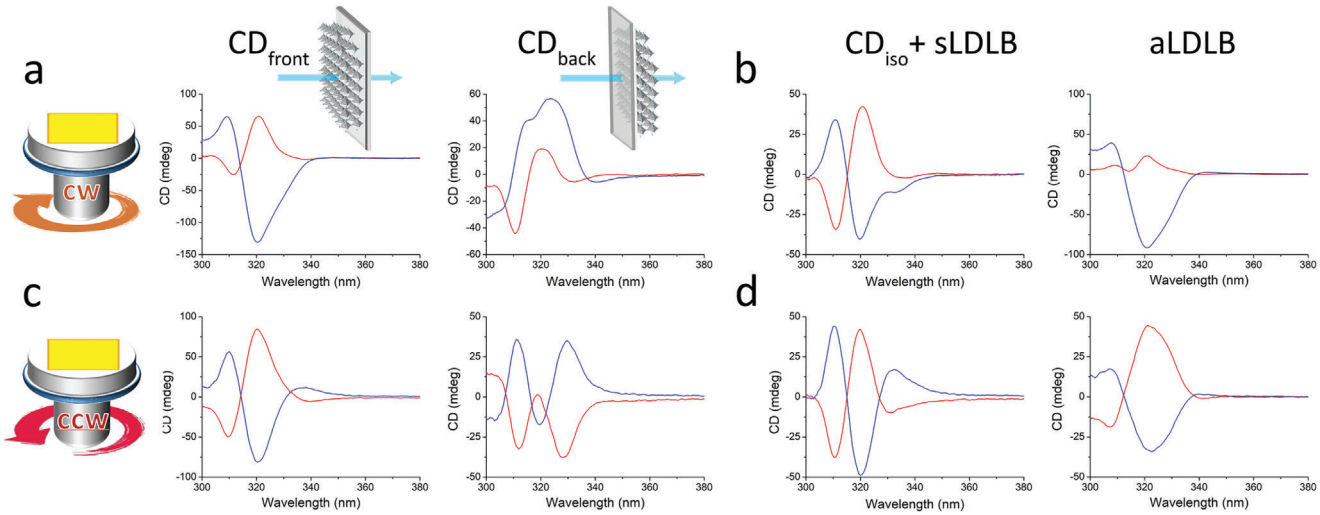

Figure 2. CD of (*S*-HP1A)$PbBr_3$ (red lines) and (*R*-HP1A)$PbBr_3$ (blue lines). a) CD measurements front and back configurations on spin-coated films prepared under clockwise rotation. b) CD_{iso} + sLDLB and aLDLB calculated from experimental measurements in (a). c,d) Same for the thin films prepared under counter-clockwise rotation.

allows to obtain accurate g_{abs} factors of $+1.10^{-3}$ and -1.10^{-3} for (*S*-HP1A)$PbBr_3$ and (*R*-HP1A)$PbBr_3$, respectively. On the other hand, the aLDLB effects present different intensities between (*S*-HP1A)$PbBr_3$ and (*R*-HP1A)$PbBr_3$, almost four times more intense in the latter. This stronger aLDLB explains the sign inversion in (*R*-HP1A)$PbBr_3$ between CD_{front} and CD_{back}, which was not observed in the compound based on the *S* enantiomer.

What is the rationale of the different aLDLB between the two enantiomers? In chiral molecules, while CD_{iso} has a pure excitonic origin, aLDLB effects in turn are related to local anisotropy and the non-alignment of LD and LB transition dipoles. In the case of crystalline thin films particularly, as for metal-halide semiconductors, epitaxial growth can be strongly dependent on sample preparation. Therefore, at this step, we hypothesized the possible impact of the spin-coating procedure, precisely the direction of the rotation during deposition (clockwise versus counter-clockwise). Indeed, as any chiral molecule or assembly can be associated to a helical potential, this rotation direction is expected to influence the supramolecular assembly of two enantiomeric compounds to a varying extent. For many years, similar mechano-chiral effects have been demonstrated in (metal-)organic compounds.[17] For example, J. M. Ribó et al. have shown the influence of rotatory evaporation of solutions for the chiral induction in porphyrin-based J-aggregates.[18] In our typical spin-coated thin film fabrication procedure, the direction of rotation was configured clockwise. Therefore, a new series of thin films of (*S*/*R*-HP1A)$PbBr_3$ was prepared, using the same precursor solutions and procedure but changing the rotation direction of the spin-coating (i.e., counter-clockwise). CD measurements for both front and back positions of the thin film strongly differ from the measurements performed with the clockwise preparation (Figure 2c). The same equations were used for the calculation of CD_{iso} + sLDLB and aLDLB (Figure 2d). The obtained CD_{iso} + sLDLB spectra mostly present the same shape and values as in the clockwise configuration, with a slight difference at lower energy (around 330 nm). This was expected due to the same chemical nature of the thin films. On the other hand, aLDLB was strongly affected by the clockwise/counter-clockwise parameter. It is rather difficult to quantitatively analyze the effect of the rotation on the intensity of these macroscopic effects, although it appeared from a large set of measurements that aLDLB tends to increase (in absolute value) for counter-clockwise rotation compared to clockwise in (*S*-HP1A)$PbBr_3$ and tends to decrease in (*R*-HP1A)$PbBr_3$. Moreover, in order to discard the possible presence of impurities that could also influence the shape of aLDLB, another set of measurements were conducted starting from another batch of organic precursors (Figure S7, Supporting Information). The consistency in the results confirmed this trend. XRPD measurements were performed for each compound and spin-coating configuration (Figure S8, Supporting Information). The strong similarity between diffractograms, with almost no difference in peak relative intensities, shows that both chemical composition and crystal orientation inside the thin films remained unchanged with sample preparation. The absolute absorbance, which was the same for all compounds (Figure S9, Supporting Information), also supports the thickness integrity among the series. On the other hand, optical microscopy images showed that the compounds presenting the strongest aLDLB signals have stronger roughness with the presence of larger crystal domains (Figure S10, Supporting Information). Such modulation with the rotation direction was not observed for the racemic compound, since the thin films prepared under both clockwise and counter-clockwise rotation present the same roughness as well as a similar and very weak aLDLB signal (Figure S11, Supporting Information). Therefore, these results suggest that the synergy between the nature of the enantiomer and spin-coating rotation direction can influence the presence and size of crystal domains, and that larger the macroscopic anisotropy, stronger could be the aLDLB effects. Such influence of the rotation direction couldn't be observed previously in thin films of organic oligomers or polymers presenting strong LDLB, and may be explained based on the different crystal growth

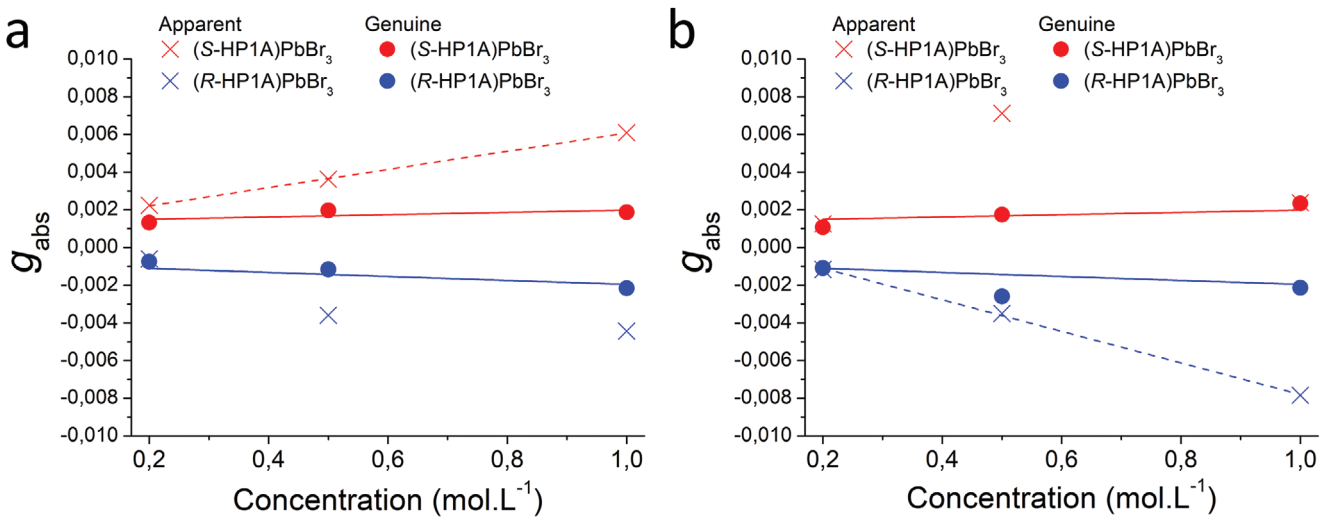

Figure 3. Concentration dependence of calculated g_{abs} factors at $\lambda = 320$ nm for (*S*/*R*-HP1A)$PbBr_3$. a) Values obtained for the clockwise spin-coating. A linear increase of apparent dissymmetry is observed for (*S*-HP1A)$PbBr_3$. b) Values obtained for the counter-clockwise configuration. A linear increase of apparent dissymmetry is observed for (*R*-HP1A)$PbBr_3$. In both cases, the calculated genuine factors are thickness-independent.

ability between organic molecules and metal-halide compounds. Indeed, while the chiral oligothiophene-based supramolecular assembly is strongly modulated by post-deposition operations such as solvent annealing,[19] the crystal growth of metal-halide on the surface usually initiates before the spin-coating process and annealing is only necessary for removing traces of solvent and improving the overall homogeneity of the crystalline film. This important difference must be the reason for the stronger influence of rotation direction in the fabrication of metal-halide thin films. Finally, starting the rotation before the deposition of the precursor solution could strongly decrease the strength of aLDLB in both films (Figure S12, Supporting Information). This further confirms that the presence of aLDLB doesn't originate from the direction of spin-coating rotation but rather from the anisotropic crystallization that initiates right after deposition of the DMF solution on the substrate. Still, the clockwise/counter-clockwise rotation strongly affects the intensity of the aLDLB, in opposite way for each enantiomeric compound. In addition, another important parameter relies on both spinning speed[20] and spinning time,[21] since it was already shown their strong influence on the thickness of the metal-halide thin film,[22] which will de facto influence the chiroptical response. These results reveal a real impact of the spin-coating parameters on the supramolecular assembly of chiral molecular materials.

At this step, the presence of the symmetric LDLB term in the CD response has not yet been investigated. According to the theory of Tempelaar et al., sLDLB is invariant upon sample flipping and should in principle give bisignate profile of the spectrum, although it has a completely different origin than the Cotton effect in CD.[12] How to experimentally discriminate between genuine CD_{iso} and sLDLB? As far as CD_{iso} is concerned, the g_{abs} factor should be independent to the film thickness l. Indeed, CD_{iso} is a single-scattering event (scaling at l) and results in the thickness-independent g_{abs} factor (CD normalized by absorbance). On the other hand, both aLDLB and sLDLB terms scale as l^2, since they are considered as double-scattering events. Therefore, the dissymmetry factors corresponding to aLDLB and sLDLB should linearly increase with sample thickness. Very recently, thickness-dependent CD studies were performed on thin films and KBr pellets of 1D and 2D chiral metal-halide compounds, however these measurements could only highlight the possible CD signal overload and absorbance saturation region.[23] In order to confirm the presence or absence of sLDLB in (*S*/*R*-HP1A)$PbBr_3$, thin films of different thicknesses were prepared and characterized. Three different concentrations of the precursor solutions have been selected (0.2, 0.5 and 1.0 M based on the formula unit). For each concentration, thin films were prepared under both clockwise and counter-clockwise rotation and CD measurements were performed as previously described (Figure S13, Supporting Information). According to surface profilometry measurements, these concentrations resulted in thin films of thicknesses of around 20, 60 and 130 nm (±10 nm and average roughness of about 5 nm) for 0.2, 0.5 and 1.0 M concentration, respectively. Nevertheless, the total and genuine g_{abs} factors (i.e., calculated with respect to front measurement and front/back semi-sum, respectively) were plot as function of the precursor solution concentrations for more accuracy (**Figure 3**). The total dissymmetry factors can be strongly modulated due to the increasing contribution of aLDLB by increasing film thickness. Although a linear increase of the total g_{abs} can be observed in some cases (as depicted by dashed lines in Figure 3), the evolution of this factor doesn't necessarily follow any function due to competing effect between CD_{iso} and aLDLB (sometimes being opposite in sign at a given wavelength) and because the aLDLB can be affected by sample preparation, such as clockwise/counter-clockwise spin-coating rotation. After averaging CD_{front} and CD_{back} measurements, the obtained dissymmetry factors are the same for the three concentrations, confirming the genuine g_{abs} values of about $+1.10^{-3}$ and -1.10^{-3} for (*S*-HP1A)$PbBr_3$ and (*R*-HP1A)$PbBr_3$, respectively. This constancy across the range of concentration also confirms the absence of thickness-dependent sLDLB in this series of thin films. It can be concluded that only CD_{iso} and aLDLB are present in the bromide-based hybrid compounds. Finally, it appears that the aLDLB effects almost vanish for the lowest concentration of 0.2 M (Figure

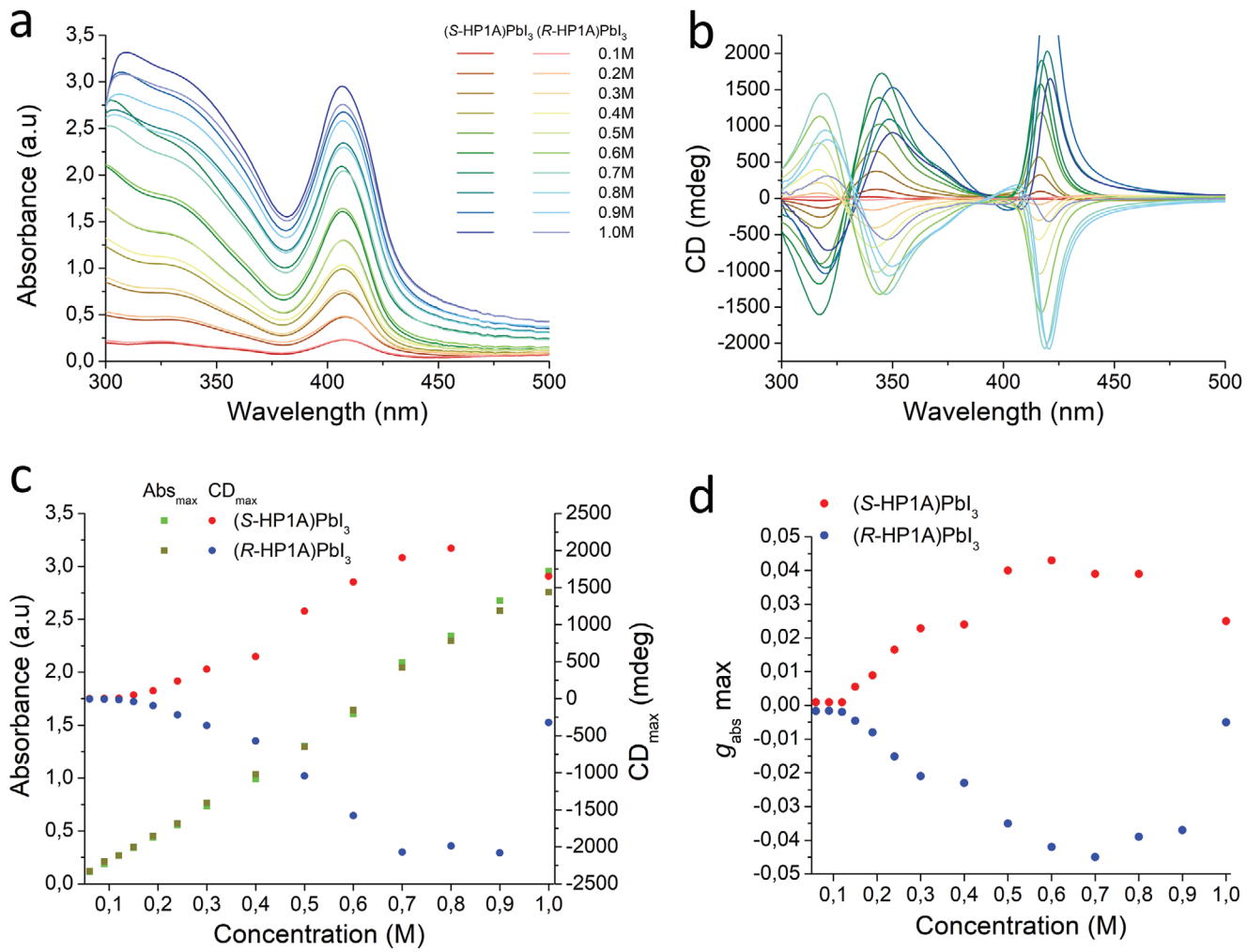

Figure 4. CD study of (*S*/*R*-HP1A)PbI_3. a) Absorbance and b) CD measurements as a function of concentration of the precursor solution. c) Concentration dependence of absorbance and CD values at 417 nm. d) Concentration dependence of g_{abs} factor.

S13, Supporting Information), proving that a pure molecular CD can be obtained under these conditions. Comparison of optical microscopy images of the different thin films further confirms the influence of crystal domain sizes in the strength of aLDLB.

Previous reports on solid-state CD of (metal-)organic materials reasonably described aLDLB as a reproducible effect rather than an experimental artefact, which allows to make use of these antisymmetric effects in practical devices.[9] However, it appears from the present measurements on (*S*/*R*-HP1A)$PbBr_3$ that aLDLB can be strongly dependent on sample preparation, pointing out the importance of describing all the selected conditions of sample preparation before reporting any dissymmetry factor. It also reveals the possibility to modulate such conditions in order to optimize the CD_{iso}/aLDLB ratio for the target application.

2.3. Chiroptical activity in (*S*/*R*-HP1A)PbI_3

Lead-iodide compounds have been reported to exhibit the strongest dissymmetry factors, usually between three and five times the values obtained with the lead-bromide counterparts. In the present example, thin films of (*S*/*R*-HP1A)PbI_3 prepared in the same conditions as (*S*/*R*-HP1A)$PbBr_3$ exhibit much stronger CD signals (reaching a degree-scale), suggesting very high dissymmetry factors in the iodide-based compounds (Figure S14, Supporting Information). With such amplitude of the CD signal, (*S*/*R*-HP1A)PbI_3 appeared to be good candidates to perform CD measurements on a series of films prepared from a large range of concentrations of the precursor solution, ranging from 0.06 to 1.0 M based on the formula unit. At each concentration, the thin films presented an excitonic peak located at 417 nm (Figure 4a). The evolution of the absolute absorbance between samples indicates a linear increase of the film thickness with the concentration and further confirms the integrity of the chemical composition. This linear increase was also suggested based on profilometry surface measurements, with a thickness range estimated at between 20 nm (at 0.2 M) and 150 nm (1.0 M). The evolution in the chiroptical response across the series is less straightforward (Figure 4b). It thus appears important to verify the presence of artefacts, aLDLB and sLDLB effects for each concentration.

For example, the thin film of (*S*-HP1A)PbI_3 prepared from a 0.3 M precursor solution (absolute absorbance of around

0.8) shows a small but measurable azimuth angle dependence on both CD and LD values (Figure S15a–b, Supporting Information). While the apparent g_{abs} factor was first estimated at +0.0229, this value was lowered to +0.0227 after artefacts corrections. It shows that the thin film presents negligible LD. Finally, as confirmed by the superposition of CD measured in both front and back positions (Figure S15c, Supporting Information), no measurable aLDLB contribution could be observed, thus confirming (at this step) the calculated g_{abs} for such concentration. We can conclude that both artefacts and aLDLB can here be disregarded. For this reason, such iodide-based thin films don't behave differently depending on the direction of the spin-coating rotation. Similarly, these corrections have been applied for all concentrations and both compounds, confirming the absence of measurable artefacts and aLDLB in the entire series of thin films. On the other hand, strong modulations both in shape and values of CD spectra could be observed for concentrations of 0.9 and 1.0 M, a clear indication of signal saturation for such high concentrations. In the range 0.06 – 0.8 M, a non-linear evolution of the maximum CD values was also observed, at the difference of the absolute absorbance (Figure 4c). Once normalized by the absorption, the values of dissymmetry factor at 417 nm were plot as function of concentration (Figure 4d). A strong evolution appeared, with an increase of g_{abs} from $\pm1.10^{-3}$ to $\pm4.10^{-2}$. The strong thickness-dependence suggests that the CD signals are dominated by sLDLB and co-exist with genuine CD_{iso} in (*S*/*R*-HP1A)PbI_3 thin films. Indeed, the g_{abs} factors for the lowest thicknesses are calculated at $+1.10^{-3}$ and -1.10^{-3} for (*S*-HP1A)PbI_3 and (*R*-HP1A)PbI_3, respectively. These constant values obtained from 0.06 to 0.12 M suggest the pure molecular origin (CD_{iso}) of the CD response. At higher concentration, the g_{abs} factor linearly increases until reaching a plateau at 0.6 M. On the other hand, the XRPD patterns (Figure S5, Supporting Information) show no variation in the shape of the diffraction peaks, nor in their associated 2Theta values, therefore the first order supramolecular arrangement was not modulated through the whole series of thin films. These results support the presence of sLDLB which increases the dissymmetry factors up to $\pm4.10^{-2}$. The results also demonstrate the saturation of the CD signal at the highest thicknesses. Finally, it should be noted that very similar results were obtained by replacing the FTO substrates for glass substrates (Figure S16, Supporting Information).

2.4. Molecular Origins of Chiroptical Activity

Surprisingly, the same values of genuine dissymmetry factors are obtained for both (*S*/*R*-HP1A)$PbBr_3$ and (*S*/*R*-HP1A)PbI_3 thin films. It is rather contradictory with previous reports that highlighted the larger CD observed in iodide compounds compared to bromide compounds, although it can now be understood that such comparative studies possibly relied on uncomplete characterizations. In addition, such studies were lacking of isostructural bromide and iodide-based compounds. For these reasons, it was challenging to study the influence of chemical and structural properties in the chiroptical activity of metal-halide semiconductors. In this context, two different hypotheses were recently proposed. On the one hand, it was suggested that the higher CD responses observed in iodide networks compared to bromide networks could be explained based on the stronger spin-orbit coupling (SOC) in iodide compounds due to the smaller exciton binding energy.[24] On the other hand, the fine modulation of the structure in nano-confined chiral perovskites suggested that the strength of hydrogen-bonding interactions between chiral cation and inorganic network could be considered as a key parameter for the chiroptical activity.[15] These two explanations on the origin of CD in metal-halide networks can be complementary. In the light of the present results, the hypothesis on intermolecular interactions seems to have more influence on the genuine CD, since the hydrogen-bonding contacts are strictly the same in both (*S*/*R*-HP1A)$PbBr_3$ and (*S*/*R*-HP1A)PbI_3. This has also been proposed to be at the origin of chirality transfer strength in a series of 2D chiral halide perovskites.[25] Nevertheless, the first hypothesis on the influence of chirality-induced SOC cannot be disregarded, and could be envisaged to slightly influence the g_{abs} values, even though it was not observed in the present compounds.

2.5. Macroscopic Effects on Chiroptical Activity

Despite the similar natural optical activity of both bromide and iodide-based hybrid compounds (with genuine g_{abs} of $\pm1.10^{-3}$), it clearly appears that the nature of the halide has a predominant role in the overall chiroptical response. Here, iodide-based compounds show an apparent dissymmetry factor of one order of magnitude higher than the bromide counterparts. As mentioned in the introduction, in the previous studies on chiroptical properties of metal-halide semiconductors, the nature of the halide (Br versus I) influenced the g_{abs} values in a lesser extent. This was due to the fact that in both bromide and iodide-based 1D networks, a non-negligible aLDLB effect was observed and the calculated g_{abs} values were comprised between 10^{-4} and 10^{-3}. To the best of our knowledge, no sLDLB effects were previously observed in chiral metal-halide semiconductors. Here, aLDLB effects could be observed only in (*S*/*R*-HP1A)$PbBr_3$, keeping the apparent dissymmetry factors in the range between 10^{-3} and 10^{-2}. On the other hand, the sLDLB effect observed in (*S*/*R*-HP1A)PbI_3 resulted in an increase of this factor up to 4.10^{-2}. The reason for different linear contributions in two isostructural compounds may be explained by a different crystal growth of the thin films. (*R*-HP1A)$PbBr_3$ and (*R*-HP1A)PbI_3 thin films displayed very similar XRPD patterns, with the presence of only (0kl) peaks that confirmed the predominant deposition of the hybrid compound with the propagation direction of the 1D chain parallel to the substrate (Figure 5a and d). However, a stronger intensity of the peaks associated to the (002) and (040) planes could be observed in (*R*-HP1A)$PbBr_3$ (highlighted in blue), as well as the presence of (051) and (071) peaks (highlighted in green). These additional peaks indicated a lower preferential orientation of the 1D chains in (*R*-HP1A)$PbBr_3$ compared to (*R*-HP1A)PbI_3 and could be at the origin of the very different thin film textures (Figure 5b and e). As mentioned in the chiroptical characterization of (*S*/*R*-HP1A)$PbBr_3$, the CD responses were associated to the presence of large crystal domains in the thin films (Figure 5c), with roughness that could be dependent on sample preparation. For (*S*/*R*-HP1A)PbI_3 however, optical microscopy images of the thin films under unpolarized and polarized light confirm the absence of such large crystal domains and

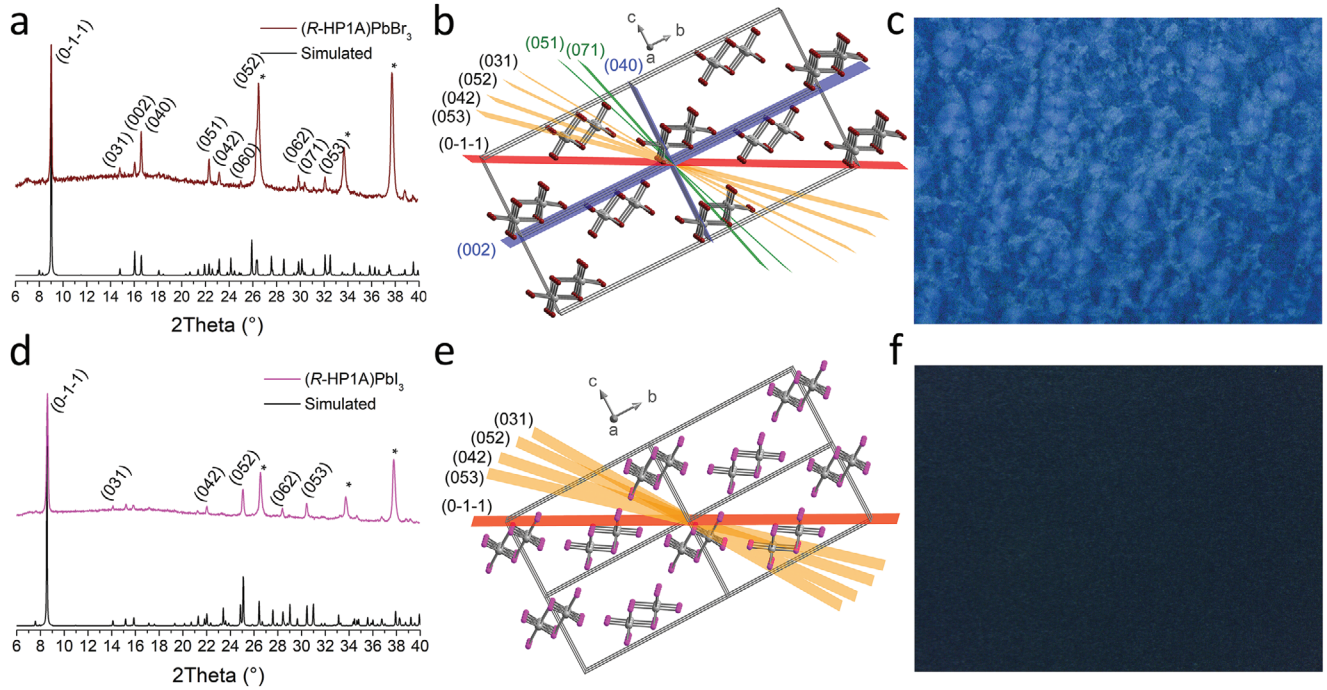

Figure 5. Thin film orientation study of (*R*-HP1A)$PbBr_3$ and (*R*-HP1A)PbI_3. a) XRPD diffraction patterns of (*R*-HP1A)$PbBr_3$ thin film with hkl planes indexation. b) View of the crystal structure of (*R*-HP1A)$PbBr_3$ highlighting the preferential orientation of the 1D chains on the substrate. c) Optical microscope image of the thin film under polarized light. d–f) Same for (*R*-HP1A)PbI_3. In (b) and (e), the hkl plane corresponding to the main (0-1-1) peak is highlighted in red, the hkl planes observed in both compounds are highlighted in orange, and the hkl planes corresponding to the peaks observed for (*R*-HP1A)$PbBr_3$ are highlighted in green and blue.

reveal an homogeneous texture of the films (Figure 5f) with a small and gradual increase of the roughness by increasing the film thickness (Figure S17, Supporting Information). In conclusion, this huge difference of CD signal observed between thin films based on isostructural compounds and prepared under the same conditions couldn't be explained based on the sole effect of SOC, but rather arises from different crystal growth and therefore different macroscopic effects inside the thin films, here leading in the case of bromide-based compounds to aLDLB effects due to large crystal domains, and to sLDLB in iodide-based compounds due to the twist angle between stacks of molecules, according to Tempelaar's model.[12] The discussion can be extended to 2D metal-halide networks. As mentioned in the introduction, 1D networks have shown dissymmetry factors of more than one order of magnitude higher than 2D based compounds. For example, the 2D chiral compounds of formula (*S*/*R*-HP1A)$PbBr_4$ displayed a g_{abs} of $\pm 10^{-4}$,[16] one order of magnitude lower that the 1D networks obtained starting from the same chiral cation. Such results were understood based on the increase of exciton broadening (due to lower quantum confinement) when increasing the dimensionality of the system.[13] However, on the basis of the new results obtained with (*S*/*R*-HP1A)$PbBr_3$ and (*S*/*R*-HP1A)PbI_3, it is strongly envisaged that not only the SOC could influence the CD strength. In layered-based metal-halide networks, the strong preferential orientation on the substrate and optimal overlap between 2D layers naturally prevents crystal domains or twist angle between stacks, and therefore prevents the generation of (antisymmetric and symmetric) LDLB effects. On the other hand, it was observed for many years that 1D metal-halide compounds can show non-homogeneous deposition on surfaces, as observed in (*S*/*R*-HP1A)$PbBr_3$. Furthermore, the results obtained with (*S*/*R*-HP1A)PbI_3 shed light on the strong effect due to the twist angle and non-homogeneous stacking of the molecules on the surface as previously rationalized by Tempelaar et al. and observed in benzo[1,2-*b*:4,5-*b*']dithiophene-based oligothiophene films.[12] Therefore, it is reasonable to conclude that 1D metal-halide networks are more interesting candidates than 2D compounds for the generation and modulation of CD strength by controlling aLDLB and sLDLB effects.

2.6. Chiroptical Activity Measurements on Metal-Halide Networks

The present results highlight the importance of measuring the chiroptical properties on thin films of various thicknesses and in various orientations for a same enantiomer. Indeed, it is crucial to analyze all possible macroscopic effects in order to perform a comparative study and conclude about the molecular origins of CD in metal-halide networks. Considering the new hypotheses, some compounds may therefore be re-investigated. For example, one of the first CD study of 1D lead-iodide networks reported a g_{abs} factor of ±0.02 (Figure S18, Supporting Information).[7] Interestingly, the compounds of formula (*S*/*R*-*α*-PEA)PbI_3 (*α*-PEA = *α*-phenylethylammonium) presented a different type of 1D network than in (*S*/*R*-HP1A)PbI_3 (single-chain of face-sharing octahedra in (*S*/*R*-*α*-PEA)PbI_3, double-chain of edge-sharing octahedra in (*S*/*R*-HP1A)PbI_3), but both compounds share similar

apparent g_{abs} factors at the given absorbance of 1 (±0.02 in (*S*/*R*-HP1A)PbI_3 at 0.4 M concentration). In the first place, these results could suggest that in 1D networks, the chiroptical properties would be influenced by the nature of the halide rather than the type of connectivity between metal-halide octahedra. By extension, one could anticipate a possible predominance of sLDLB in the CD responses of (*S*/*R*-*α*-PEA)PbI_3, such as it was observed in (*S*/*R*-HP1A)PbI_3. However, such assumptions will be strongly revised after a careful comparative study. Despite proper preparation conditions of (*S*/*R*-*α*-PEA)PbI_3 thin films (precursor solution at 0.3 M, discarding any possible saturation of the CD signal) and the highly preferred orientation of the 1D chains as observed by XRPD, crystal domains were observed from optical microscopy images under polarized light. The authors also mentioned the possible presence of LD and LB due to a slight modulation of the CD response at different azimuth angle measurements. Still, the presence or absence of aLDLB couldn't be confirmed since the measurements were performed for only one position (front or back) of the thin film. On the other hand, thickness-dependence measurements were not performed in order to discriminate between molecular CD and sLDLB. More recently, H. Lu et al. reported the crystal structure and solid-state CD of (*R*-EBA)PbI_3 (EBA = ethylbenzylammonium), which is isostructural to (*S*/*R*-*α*-PEA)PbI_3 due to the similarity in the cation structure (Figure S18a, Supporting Information).[13] Interestingly, optical microscopy images of the film with crossed-linear polarizers revealed a similar aspect than in (*S*/*R*-*α*-PEA)PbI_3 thin films with large crystal domains. The chiroptical activity of (*R*-EBA)PbI_3 was analyzed in more details, showing strong aLDLB that could invert the CD response upon sample flipping. After extracting the aLDLB contribution from the apparent CD signal, the calculated g_{abs} factor in (*R*-EBA)PbI_3 was found at around -7.10^{-4} at all thicknesses, demonstrating that the authors could disclose the pure molecular chirality of the material. It is therefore strongly envisaged that the strong CD responses obtained in the isostructural (*S*/*R*-*α*-PEA)PbI_3 compounds were mainly altered by the presence of antisymmetric LDLB, at the difference of the predominant sLDLB in thin films of (*S*/*R*-HP1A)PbI_3. The observation of such different behaviors between two systems with similar chemical composition, which differ only by the organic cation used and the shape of the inorganic chain, further support the importance of hydrogen-bonding interactions between chiral organic cation and metal-halide network. A complete study on a large number of metal-halide networks would be necessary in order to reveal the relative contribution of molecular and macroscopic features on the ratio of CD/aLDLB/sLDLB, and to fully describe the polarization ability of 1D chiral metal-halide semiconductors.

Through all these considerations, a guide for measuring CD of chiral metal-halide semiconductors with total accuracy can now be provided. To be fully validated, the g_{abs} value must be reported for thin films prepared from non-saturated precursor solutions. The absence of artefacts must be controlled by performing measurements at various azimuth angles. More importantly, the presence/absence of aLDLB must be confirmed by flipping the film and comparing both front and back positions measurements. In the case of predominant aLDLB over CD_{iso}, as observed in 1D lead-bromide networks, changing the direction of the rotation during the spin coating process can strongly modulate the CD_{iso}/aLDLB ratio. This effect can be strongly minimized in the case of highly oriented thin films, which can be demonstrated by XRPD and the absence of crystal domains by polarized optical microscopy images. The CD_{iso} or sLDLB nature of the chiroptical response can only be confirmed by the preparation and characterization of various thin films of different thicknesses, i.e., starting from different concentrations of the precursor solutions. Finally, to be fully reproducible, experimental procedures should describe all sample preparation parameters (duration of spin-coating, rpm speed), including the clockwise or counter-clockwise rotation during the spin-coating process.

3. Conclusion

The synthesis and experimental chiroptical study of new lead-halide 1D networks could demonstrate the strong impact of macroscopic interferences in the solid-state CD signals. The possibility to synthesize isostructural compounds that only differ from the nature of the halide (Br versus I) was critical in order to observe the different linear effects and to reveal their macroscopic origins. It also allowed to disclose the pure molecular CD (CD_{iso}), which is inherently thickness-independent, from the antisymmetric and symmetric LDLB effects. The discrimination between aLDLB and sLDLB is straightforward since these effects differ from their variance and invariance upon sample flipping, respectively. Therefore, aLDLB contribution can be isolated after sample flipping, while performing the measurements on thin films of various thicknesses allows to discriminate between sLDLB and CD_{iso}. A thickness-independent g_{abs} factor proves the predominance of CD_{iso} in the thin film. On the other hand, if a gradual increase of the dissymmetry factor is still observed after artefacts and aLDLB corrections, this demonstrates that the chiroptical properties are sLDLB in nature and originate from the helical stacking of a transition dipole. These results lead the possibility to re-investigate previous CD measurements of metal-halide networks. In combination with previous results, a trend in the chiroptical origins of metal-halide semiconductors can be observed, although it sometimes relies on uncomplete chiroptical measurements. This study demonstrates the importance of controlling the possible artefacts and LDLB contributions to get the real CD signature of a chiral metal-halide network. It also reveals the optimal preparation conditions as well as the characterization measurements necessary for a complete chiroptical study. Such methodology should be applied in a large range of hybrid networks in order to quantitatively analyze the impact of both exciton binding energy and intermolecular interactions on the chiroptical performances of this important family of hybrid materials.

Supporting Information

Supporting Information is available from the Wiley Online Library or from the author.

Acknowledgements

The work in France was supported by the CNRS and the University of Angers.

Conflict of Interest

The author declares no conflict of interest.

Data Availability Statement

The data that support the findings of this study are available from the corresponding author upon reasonable request.

Keywords

circular dichroism, chirality, chiroptical activity, perovskites, metal-halide

Received: February 9, 2024
Revised: May 7, 2024
Published online: May 25, 2024

[1] J. Ahn, E. Lee, J. Tan, W. Yang, B. Kim, J. Moon, *Mater. Horiz.* **2017**, *4*, 851.
[2] Z. N. Georgieva, Z. Zhang, P. Zhang, B. P. Bloom, D. N. Beratan, D. H. Waldeck, *J. Phys. Chem. C* **2022**, *126*, 15986.
[3] C.-Y. Chai, Q.-K. Zhang, C.-Q. Jing, X.-B. Han, C.-D. Liu, B.-D. Liang, C.-C. Fan, Z. Chen, X.-W. Lei, A. Stroppa, R. O. Agbaoye, G. A. Adebayo, C.-F. Zhang, W. Zhang, *Adv. Optical Mater.* **2023**, *11*, 2201996.
[4] C. Yuan, X. Li, S. Semin, Y. Feng, T. Rasing, J. Xu, *Nano Lett.* **2018**, *18*, 5411.
[5] H. Lu, Z. Valy Vardeny, M. C. Beard, *Nat. Rev. Chem.* **2022**, *6*, 470.
[6] Y. Dang, X. Liu, Y. Sun, J. Song, W. Hu, X. Tao, *J. Phys. Chem. Lett.* **2020**, *11*, 1689.
[7] C. Chen, L. Gao, W. Gao, C. Ge, X. Du, Z. Li, Y. Yang, G. Niu, J. Tang, *Nat. Commun.* **1927**, *2019*, 10.
[8] A. Ishii, T. Miyasaka, *Sci. Adv.* **2020**, *6*, eabd3274.
[9] G. Albano, G. Pescitelli, L. Di Bari, *ChemNanoMat* **2022**, *8*, 202200219.
[10] M. Wolffs, S. J. George, Ž. Tomović, S. C. J. Meskers, A. P. H. J. Schenning, E. H. Meijer, *Angew. Chem., Int. Ed.* **2007**, *46*, 8203.
[11] G. Albano, M. Lissia, G. Pescitelli, L. A. Aronica, L. Di Bari, *Mater. Chem. Front.* **2017**, *1*, 2047.
[12] A. Salij, R. H. Goldsmith, R. Tempelaar, *J. Am. Chem. Soc.* **2021**, *143*, 21519.
[13] Z. Zhang, Z. Wang, H. H.-Y. Sung, I. D. Williams, Z.-G. Yu, H. Lu, *J. Am. Chem. Soc.* **2022**, *144*, 22242.
[14] J. Hao, H. Lu, L. Mao, X. Chen, M. C. Beard, J. L. Blackburn, *ACS Nano* **2021**, *15*, 7608.
[15] S. Ma, Y.-K. Jung, J. Ahn, J. Kyhm, J. Tan, H. Lee, G. Jang, C. U. Lee, A. Walsh, J. Moon, *Nat. Commun.* **2022**, *13*, 3259.
[16] A. Abhervé, N. Mercier, A. Kumar, T. K. Das, J. Even, C. Katan, M. Kepenekian, *Adv. Mater.* **2023**, *35*, 2305784.
[17] J. Crusats, Z. El-Hachemi, J. M. Ribó, *Chem. Soc. Rev.* **2010**, *39*, 569.
[18] J. M. Ribó, J. Crusats, F. Sagués, J. M. Claret, R. Rubires, *Science* **2001**, *292*, 2063.
[19] G. Albano, M. Górecki, G. Pescitelli, L. Di Bari, T. Jávorfi, R. Hussain, G. Siligardi, *New J. Chem.* **2019**, *43*, 14584.
[20] G. Albano, F. Salerno, L. Portus, W. Porzio, L. A. Aronica, L. Di Bari, *Chem. Nano. Mat.* **2018**, *4*, 1059.
[21] R. Munir, A. D. Sheikh, M. Abdelsamie, H. Hu, L. Yu, K. Zhao, T. Kim, O. El Tall, R. Li, D.-M. Smilgies, A. Amassian, *Adv. Mater.* **2017**, *29*, 1604113.
[22] Z. Wu, P. Yan, S. Hu, B. Yang, C. Wang, C. Xiang, H. Li, C. Sheng, *Opt. Mater.* **2023**, *142*, 114102.
[23] X.-B. Han, W. Wang, M.-L. Jin, C.-Q. Jing, B.-D. Liang, C.-Y. Chai, R.-G. Xiong, W. Zhang, *Anal. Chem.* **2023**, *95*, 16201.
[24] Z.-G. Yu, *J. Phys. Chem. Lett.* **2020**, *11*, 8638.
[25] J. Son, S. Ma, Y.-K. Jung, J. Tan, G. Jang, C. U. Lee, J. Lee, S. Moon, W. Jeong, A. Walsh, J. Moon, *Nat. Commun.* **2023**, *14*, 3124.